

Aerosol hygroscopic models based on in situ measurements and lidar retrievals

DANIELA VIVIANA VLADUTESCU, YONGHUA WU, BARRY GROSS, LEONA CHARLES,
FRED MOSHARY, SAMIR AHMED
Electrical Engineering Department
City College of the City University of New York
140th Street @ Convent Ave, The Grove School of Engineering, T 553
USA

<http://www-ee.cuny.cuny.edu/wwwa/web/vlad/index.html>

Abstract: - The affinity of aerosol particles to water, as measured by the relative humidity, plays an important role in several processes. It influences visibility reduction in the atmosphere, modifies aerosol gas chemistry through multiphase reactions, modifies the particles ability to act as cloud condensation nuclei resulting in an influence on the Earth's radiation budget. In this paper, we examine the modeling needed to quantify optical scattering coefficients on physical models. The model uses as input hygroscopic growth factors, refractive indexes and dry air densities measured by Hanel(1976). The relative humidity was obtained from the water vapor mixing ratio obtained using the Raman lidar located at CCNY(City College of the City University of New York) and compared with the radiosonde measurements located at Brookhaven National Laboratory . The hygroscopic model results are then compared with CCNY lidar retrievals for validation.

Key-Words: - Raman lidar, hygroscopic aerosol, hygroscopic growth factor,

1 Introduction

Aerosols can have their optical properties modified in the presence of water vapor with different classes of aerosols being modified in different manners. The need to identify hygroscopic properties from measurements is complicated by the fact that most dramatic effects occur at high relative humidity values which are not often seen at surface level but are manifested near clouds. Therefore lidar measurements near cloud base offer a chance at looking at hygroscopic properties. In particular, the ability of multiwavelength Raman lidar of performing simultaneous atmospheric measurements at three different wavelengths 355nm,1064nm and 407nm (Raman water vapor) provides the opportunity of isolating the hygroscopic effect from the number of density variations which plague the single channel approach since the normalized backscatter (to the dry state) retrieved at 355nm and 1064nm is independent of the total number of particles (for small spatial ranges). In particular, we investigate the possibility of using the ratio optical scatter measurements which eliminate the inherent problem of variable particle number and illustrate the sensitivity of different hygroscopic aerosols to these measurements and find that combining both extinction and backscatter with color ratios improves the accuracy of the retrieval

2 Aerosol Hygroscopicity

2.1 Mathematical Modeling

Hygroscopic models are a suitable way of quantitatively and qualitatively evaluate the backscatter outputs of lidars and other instruments that measure hygroscopic properties of aerosols [1,2].

The models created here are designed to determine both the color ratio of backscatter signals at 355nm and respectively 1064nm as function of altitude as well as the extinction – backscatter ratio at 355nm. It is expected that a combination of both ratios can provide improved retrieval of hygroscopic model parameters. The theory behind the model can be described by ratio of the normalized backscatter at two different wavelengths as given in equation 1 [3,4].

$$\frac{\bar{\beta}_1}{\bar{\beta}_2} = \frac{\left(\frac{\sigma_s(RH)}{\sigma_{s0}}\right)_1}{\left(\frac{\sigma_s(RH)}{\sigma_{s0}}\right)_2} = \frac{\int \left[Q\left(\frac{2\pi r}{\lambda}, m\right) * N_s * \frac{dr(r)}{d\log r} * \pi^2 \right] d\log r}{\int \left[Q\left(\frac{2\pi r_0}{\lambda}, m_0\right) * N_s * \frac{dr(r_0)}{d\log r_0} * \pi_0^2 \right] d\log r_0} \quad (1)$$

The bar in equation 1 stands for normalization of the backscatter of the wet particle (at a given relative humidity) with respect to the backscatter of the same particle in dry state.

In the above equation, r is the equivalent radius of the wet particle, r_0 is the radius of the dry particle, Q is the backscattering efficiency, λ is the wavelength, m is the refractive index $n(r)$ is the number density (number of particles per volume) and $\frac{dn(r)}{d \log r}$ is the

aerosol size distribution.

The models are based on measured dry particle densities [7] with their corresponding real and imaginary refractive indexes at different wavelengths. The radius and the real and imaginary refractive indexes used in the above relation are relative humidity dependent and are described by the following relations derived by Hanel [7]:

$$r = r_0 \left(1 + \frac{\rho_0}{\rho_w} \mu(RH) \frac{RH}{1-RH} \right)^{1/3} \quad (2)$$

$$n = n_w + (n_0 + n_w) \left(1 + \frac{\rho_0}{\rho_w} \mu(RH) \frac{RH}{1-RH} \right)^{-1} \quad (3)$$

$$k = k_w + (k_0 - k_w) \left(1 + \frac{\rho_0}{\rho_w} \mu(RH) \frac{RH}{1-RH} \right)^{-1} \quad (4)$$

In the above 6 to 8 relations RH represents the relative humidity, $\mu(f)$ is the linear increase coefficient, ρ_0 and ρ_w represent the dry air and water vapor density respectively, n_0 n_w represent the real refractive index of dry particles and water vapor respectively, and the imaginary refractive indexes of dry air and water vapor are represented by k_0 and k_w respectively. We note that for a given aerosol size distribution mode, the ratio eliminates the vertical concentration effects.

Using relations (2-4) in the backscatter ratio formula (1), one can identify the dry state aerosol by constructing a table of ratio scattering properties for different models and dry state conditions as a function of the RH. While the models are not extensive in the literature, we hope the models capture some of the real life behavior of different types of atmospheric aerosols (different combinations of atmospheric gases and particulates or particulates alone) under different atmospheric conditions (humidity, temperature, particle density et leave two blank lines between successive sections as here.

3 Analyses and results

The analyses of the hygroscopic properties of the aerosols have been made for the day of September 25, 2006 due to the low cloud presence in the planetary boundary layer and the expected increase relative humidity with height. In particular, the low clouds allow us to have a fairly stable atmospheric state which can be probed vertically to high RH. An example has been plotted in figure one.

Logarithm(e) of Pz^2 at 1064-nm, Sep25,2006 CCNY

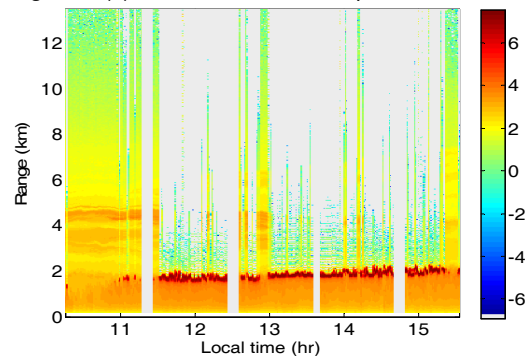


Fig. 1. Lidar image at the 1064nm on September 25th,2006

The relative humidity retrieved from the lidar water vapor channel and radiosonde temperature profile and calibrated by methods described in section II.1 and [11] is plotted in fig 2.

The local surface measurements obtained from a GPS instrument confirm the 39%-40% relative humidity at the ground agreeing quite well to the lidar measurments. The relative humidity obtained this way is then used in combination with the lidar returns at 355nm and 1064nm to determine aerosol hygroscopic properties.

The signal has been analyzed only below 2.5 km due to the low signal returns above this height.

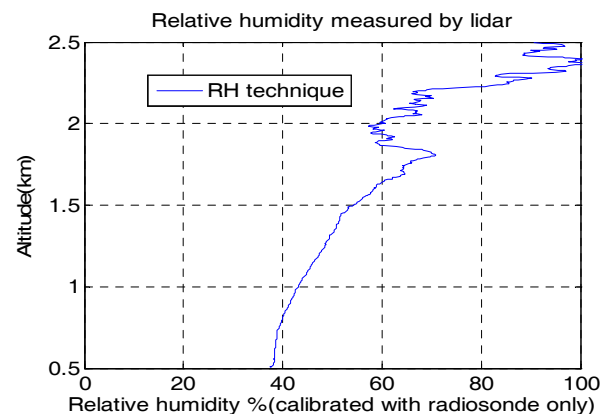


Fig. 2. Relative humidity vs. altitude

III.1 Aerosol Hygroscopicity. Comparison of lidar measurements to existing models

By performing ratios of the normalized backscatter ratio, the number concentration of particles in the atmosphere is cancelled as seen from formula (1). Therefore, we may perform vertical profile analysis on the scattering ratios without concern for the actual number density of the scattering objects in the backscattering ratio dependence of relative humidity. Using conventional lidar algorithms to determine the backscatter at 355nm and 1064nm [4,5] one can obtain the ratio of the two obtained backscattered profiles at the two wavelengths as described by (1). Preliminary results of the models normalized backscatter ratio have been plotted in fig 3. In this figure the normalized backscatter ratios of the 355nm backscattering to the 1064nm backscattering have been plotted for models 1,3,5,6 [7] and CCNY model retrieved from the vertical profiles measured by the multiwavelength Raman lidar. A description for each model is found in Hanel and described again for convenience: model 1 is represented by average aerosol in summer 1966 at Mainz, model 2 by sea-spray aerosol, model 3 by maritime aerosol over Atlantic, 13-16 April 1969, model 4 Maritime aerosol over Atlantic containing Saharan dust, 16-25 April 1969, model 5 Urban aerosol at Mainz in January 1970, model 6 Aerosol on top of the Hohenpeissenberg, elevation 1000m above MSL in the foothills of the Alps, in summer 1970 Models 2 and 4 have not been used for comparison due to the lack of information in the measured data by the author of the paper[7].

As it can be noticed the measurement data is best matched to model 3 which seems to indicate a maritime aerosol which is consistent with sea-breeze conditions observed.

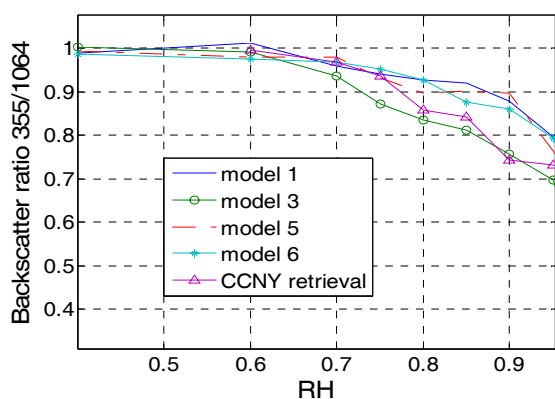


Fig. 3. Normalized aerosol backscatter ratio of the 355nm and 1064nm lidar returns

Modeling based on measured parameters

As noted above the hygroscopic models presented in this paper have been based on the measurements performed by Hanel (1976). The existing values for dry particles densities, linear mass increase coefficient and mass of water to mass of dry substance ratios have been used for each corresponding relative humidity value for each model to synthetically determine the ratio of optical scattering. The temperature used for the models was 20°C and the corresponding water vapor density is calculated for this temperature based on the relative humidity indicated by Hanel et al. for each individual mass of water vapor to mass of dry

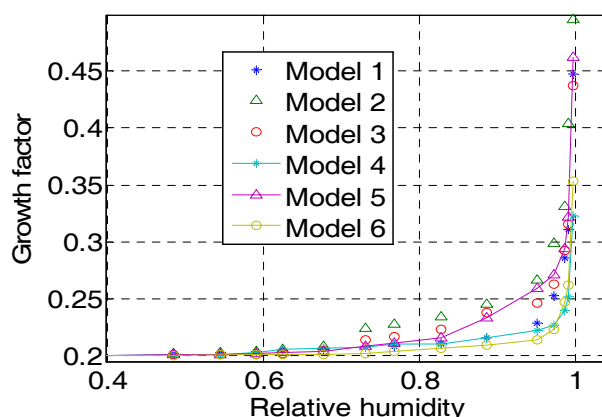


Fig. 4 Growth factor for the 6 atmospheric models with a dry radii of 0.2µm

substance and linear mass increase coefficient which are used in relations (2-4). To begin, we plot in fig 4, the particles hygroscopic radius growth for a dry

particle radius of 0.2µm for the six different models described above showing that unless the RH > .8, very little change is seen in the models. Once the microphysical model parameters are estimated, the aerosol backscatter normalized with respect to the dry particles backscatter can be calculated using equation 5.

The results obtained using equation 1 have been plotted in fig.5. The two plots represent the logarithm of two normalized ratios from equation 1 as function of model number and radii. In fig.5a has been represented the logarithm of the ratio of normalized backscatter at 1000nm to the normalized backscatter at 300nm, $\log_{10}(\bar{\beta}_{1064}(fH=.95)/\bar{\beta}_{355}(fH=.95))$, while in fig.5b. has been plotted the normalized backscatter to extinction ratio at 355nm, $\log_{10}(\bar{\beta}_{355}(fH=.95)/\bar{\alpha}_{355}(fH=.95))$. The bar means the quantity is normalized to the dry state value.

Our space of admissible is represented by the 54 cells (6 models x 9 dry radii ranging from 0.2µm to 1µm and logarithmic standard deviation is kept constant at 1.2µm since the mode width has a much weaker effect on the hygroscopic effects..

When examining the results, we note a significant variation seen between models and the different ratio types. Unfortunately, the plethora of atmospheric states behaviors is so rich that determination of a particular model for a given data set is quite a task and requires in essence large statistical data sets which can be tracked to a particular source to make any real assessment of a particular model. To this end, we content ourselves in exploring the sensitivity of the scattering measurements to the underlying hygroscopic parameters

Multiwavelength inversion of hygroscopic models and dry state radii

Considering the significant variation that can occur between models and the different ratio types, we propose here an inversion approach using multiple channels at variable RH levels to provide information in disentangling the size and hygroscopic properties. To assess this possibility, we need to fix our approach for inversion which can be simply described as a brute force identification of all possible states satisfying all possible scattering combinations within a particular measurement sensitivity.

To begin, we calculate the optical backscatter coefficients for each radii index (i_0) and aerosol model index (j_0) at all RH levels for a particular ratio k . We can then determine the inversion set as the set that satisfies all backscatter measurements simultaneously. In mathematical terms, the set of admissible solutions is obtained by determining all states indices that satisfy “all” optical coefficient constraints where R is a particular ratio of optical coefficient

$$S(i_0, j_0) \equiv \left\{ (i, j) \text{ s.t. } \frac{[R_k(i_0, j_0) - \bar{R}_k(i, j)]}{R_k(i_0, j_0)} \leq \varepsilon_k \right\} \quad (5)$$

In these calculations, the ratios R are a combination of two channel optical coefficient ratios as seen in equations 5 and 11.

$$R \equiv \left[\frac{\alpha_{355}(RH)/\beta_{355}(RH)}{\alpha_{355}(RH_0)/\beta_{355}(RH_0)} \right] \rightarrow \left[\frac{\alpha_{355}(RH)}{\alpha_{355}(RH_0)} \right] \left[\frac{\beta_{355}(RH_0)}{\beta_{355}(RH)} \right]$$

To calculate the ratio constraint error, we use the

propagation of errors using noise assumptions on the optical coefficients. Considering independence of the optical coefficient errors, the combined error for ratio R can be written as a RMS sum of the individual channel errors as

$$\varepsilon = \sigma_R = \sqrt{\sigma_{\alpha,355}^2 + \sigma_{\beta,355}^2}$$

where the assumed uncertainties are provided in table I. Once the set is constructed, we can define a metric describing the size of the retrieval set as $P(i_0, j_0) = size(S(i_0, j_0))/total \text{ number of states}$

$$\log_{10} \frac{\bar{\beta}_{1064}(fH = .95)}{\bar{\beta}_{355}(fH = .95)} \quad \log_{10} \frac{\bar{\beta}_{355}(fH = .95)}{\alpha_{355}(fH = .95)}$$

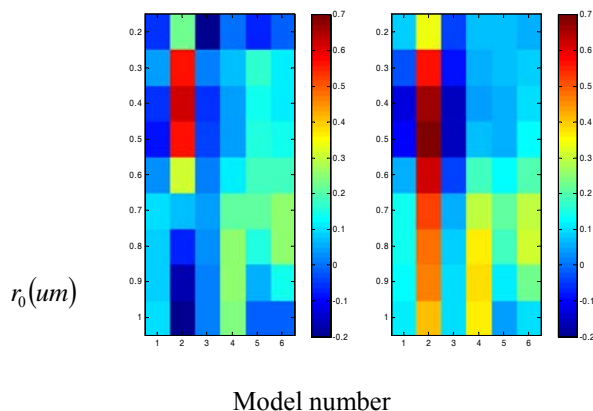


Fig. 5. a) Normalized color ratio(355nm to 1064nm) for six atmospheric models, b) Normalized lidar ratio for six atmospheric models and radii from 0.2 to 1µm

Clearly, the smaller the fraction of states that can be mistaken for the reference state P is, the better the retrieval. In figures 6 and 7, we plot the probability metric as a function of dry state radius and model number using two possible ratio schemes. All cases include the use of two high RH levels (80% and 95%).

After setting the constraints as described above, we see in fig 6 that the fraction of atmospheric states that seem to be the least ambiguous belong to the sea-spray aerosol model which makes the identification of this state most likely,. As explained before the bar used in $\bar{\beta}_{1064}/\bar{\beta}_{355}$ stands for normalized to dry state, meaning that both backscatter and extinction at 355nm have being estimated at 95% RH and then normalized to backscatter / extinction of particles in the dry state, (i.e 40% RH).

TABLE 1. INDIVIDUAL CHANNEL UNCERTAINTIES

Optical Ratio	$\alpha_{355}(RH)$	$\beta_{355}(RH)$	$\beta_{1064}(RH)$	$\beta_{2300}(RH)$
	$\alpha_{355}(RH_0)$	$\beta_{355}(RH_0)$	$\beta_{1064}(RH_0)$	$\beta_{2300}(RH_0)$
Uncertainty	20%	20%	5%	25%

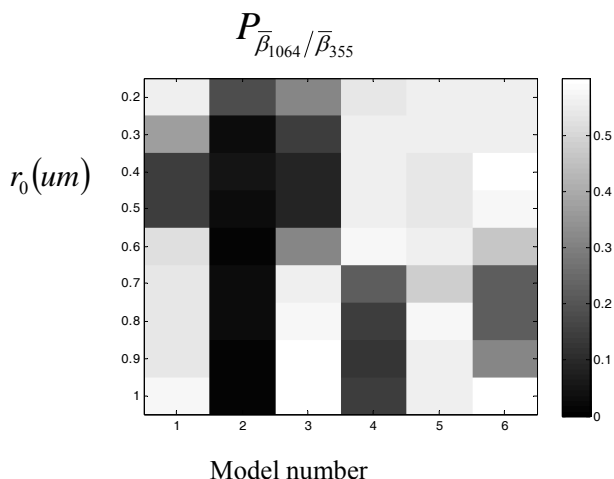


Fig. 6. Probability metric as a function of the ratio of normalized backscatter at 1064nm to normalized backscatter at 355nm for different atmospheric states (model and radii) at 80% and 95% relative humidity

In fig.7 the constraint has been forced on the ratio of normalized backscatter at 355nm to normalized extinction at 355nm (meaning normalized to backscatter of the particles in dry state at the corresponding wavelengths).

An inversion sensitivity comparison between fig. 6 and fig.7 indicates the lidar ratio constrain in fig. 7 performing better than the color ratio constrain in fig. 6.

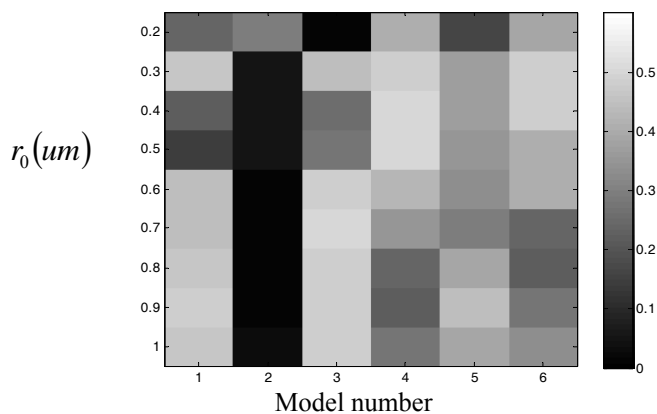


Fig. 7. Probability metric as a function of the ratio of normalized backscatter at 355 to normalized extinction at 355nm for different atmospheric states (model and radii) at 80% and 95% relative humidity.

In fig. 8 , we plot the probability metric using a combination of measurements to include both S ratio and color ratio constraints for the combinations of relative humidity already defined earlier. By forcing the unknown atmospheric state to undergo restrictions from all four constraints (UV ratio at 80% and 95%, and UV-NIR color ratio at 80% and 95% simultaneously) simultaneously the probability of mistaking the unknown state for other states than the correct one is much smaller as seen in fig.8.

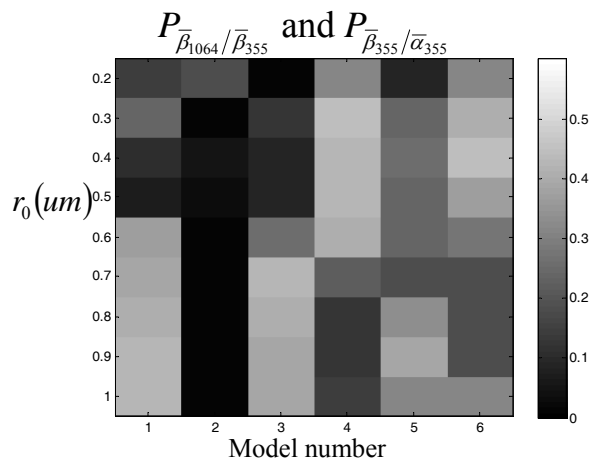


Fig. 8. Probability metric as a function of lidar and color ratio at 80% and 95% relative humidity

4 Conclusion

In this paper, we explore the possibility of determining the nature and variability of urban aerosol hygroscopic properties using multi-wavelength Raman lidar measurements at 355nm, as well as backscatter measurements at 532nm and 1064nm. The addition of these longer wavelength channels allow us to more accurately validate the homogeneity of the aerosol layer as well as provide additional multiwavelength information that can be used to validate and modify the aerosol models underlying the hygroscopic trends observed in the Raman channel. The results of the model analysis taken at wavelengths 355nm and 1064nm (those nearest our experimental arrangement) indicate a clear dependence of the backscattering and total geometric cross section on relative humidity which we observe to be in qualitative agreement with sea breeze conditions. In addition, a sensitivity analysis was performed which showed that a combination of S ratio and color ratio data should improve hygroscopic model assessment. More mathematical investigations of the new proposed analyses should be performed on the lidar data to determine the degree of agreement of the measurements to the

theoretical models based on the different models inputs. Results indicate that both S ratio and color ratio measurements can be used to constrain and identify hygroscopic models. Preliminary measurements taken under sea breeze conditions seem to indicate that the color ratio dependence on RH is qualitatively consistent with all trial theoretical models and a best match is seen for maritime aerosol model. Further efforts are needed to update the aerosol hygroscopic models. This together with more data together with back trajectory analysis is needed to develop a suitable climatology of hygroscopic aerosols. Further validation using a ground based multiwavelength nephelometer, TSI SMPS (Scanning Mobility Particle Sizer spectrometers) and TEOM (Tapered Element Oscillating Microbalance) for model updates will also be explored. For integrated total refractive index and radius distribution will be considered the Aeronet sunphotometer readings.

References:

- [1] J.M. Wallace, P.V. Hobbs, *Atmospheric Science An introductory survey*, Second edition, Academic Press Elsevier , 209-262, 2006
- [2] R. Measures, *Laser Remote Sensing: Fundamentals and Applications*, Krieger Publishing Company, Reprint Edition ,1992
- [3] A. Ansmann, U. Wandinger, M. Riebesell, C. Weitkamp and W. Michaelis, “*Independent measurement of extinction and backscatter profiles in cirrus clouds by using a combined Raman elastic-backscatter lidar*”, Applied Optics, Vol. 31, No. 33, 1992
- [4] F. G. Fernald, ”Analyses of atmospheric lidar observations: some comments”, Applied Optics, vol. 23, no. 5 , 1984
- [5] C. Weitkamp, *LIDAR range-resolved optical remote sensing of the atmosphere* , Springer, pp.100-190, 2005
- [6] D. V. Vladutescu, Y. Wu, L. Charles, B. Gross, F. Moshary, S. Ahmed, “*Analyses of Raman lidar calibration techniques based on water vapor mixing ratio measurements*”, WSEAS Trans. on Syst., vol. 2, issue 4, pp. 651–658, Apr. 2007
- [7] G. Hanel , “*The properties of Atmospheric aerosol particles as functions of the relative humidity at thermodynamic equilibrium with the surrounding moist air*”, Adv. Geophy., vol. 19, pp. 73-188 , 1976